Efficiency Evaluation of Five-Phase Outer-Rotor Fault-Tolerant BLDC Drives under Healthy and Open-Circuit Faulty Conditions

Ramin Salehi ARASHLOO, Mehdi SALEHIFAR, Harold SAAVEDRA, Jose Luis ROMERAL MARTINEZ
Electronic Engineering Department, Politechnical University of Catalunya - Barcelonatech
ramin.salehi@mcia.upc.edu

***Abstract*—Fault tolerant motor drives are an interesting subject for many applications such as automotive industries and wind power generation. Among different configurations of these systems, five-phase BLDC drives are gaining more importance which is because of their compactness and high efficiency. Due to replacement of field windings by permanent magnets in their rotor structure, the main sources of power losses in these drives are iron (core) losses, copper (winding) losses, and inverter unit (semiconductor) losses. Although low amplitude of power losses in five-phase BLDC drives is an important aspect for many applications, but their efficiency under faulty conditions is not considered in previous studies. In this paper, the efficiency of an outer-rotor five phase BLDC drive is evaluated under normal and different faulty conditions. Open-circuit fault is considered for one, two adjacent and two non-adjacent faulty phases. Iron core losses are calculated via FEM simulations in Flux-Cedrat® software, and moreover, inverter losses and winding copper losses are simulated in MATLAB® environment. Experimental evaluations are conducted to evaluate the efficiency of the entire BLDC drive which verifies the theoretical developments.**

***Index Terms*—motor drives, brushless motors, permanent magnet motors, variable speed drives, energy conservation.**

I. INTRODUCTION

Regarding their high efficiency and compactness, permanent magnet (PM) motors are gaining more interest in the field of electrical and hybrid electrical vehicles. Absence of field windings and rotor currents in PM motors not only reduces the required maintenance, but also increases the motor efficiency and its robustness [1-2].

The efficiency of an electric drive directly depends on the generated losses of its inverter block and electric motor. In the inverter block, the main sources of power loss are related to inverter snubbers and semiconductors. However, in many IGBT based topologies, it is not necessary to implement snubbers, and as a result, power losses can be categorized as IGBT and diode conduction losses, IGBT and diode off-state losses and IGBT switching losses. Among these categories, switching losses are the most important type of losses in the inverter block.

Switching algorithm has also an important impact on the final losses of inverter block. Different modulation strategies are proposed in literature to improve quality of converter outputs. These modulation methods can be categorized in two main groups including space vector modulation (SVM), and carrier based (CB) pulse width modulation (PWM) [3-4]. SVM methods let us to have a better utilization of dc bus. On the other hand, CB methods (equivalent to SVM algorithms) are easier to implement.

The second important source of drive losses is the electrical motor. During the last two decades, many controlling algorithms have been proposed in literature to minimize the motor losses by adapting machine flux to the load. These algorithms can be generally divided in three categories.

In the first category motor power factor [5] or rotor slip frequency [6] is controlled. Control of motor power factor is a practical choice for industrial drives as there is no need to speed or load information, and moreover, its adaptation is relatively fast (1 s). On the other hand, to control the rotor slip, it is required to know both speed and load information.

In the second category, the output power of the drive is kept constant and motor flux is adapted to reduce the input power of the machine [7]. However these methods are usually accompanied by several disadvantages. For example, precise load information is always required in their algorithms, and the adaptation period of these methods is quite long (7 s) [8]. In addition, a continuous disturbance can be observed in generated electrical torque. As a result, this category of efficiency improvement methods is not very popular in industrial applications.

In the third category, efficiency optimization methods are directly based on the loss model of electrical motor. These methods can be easily combined by field oriented controlling (FOC) algorithms which are already based on machine´s knowledge [9]. Although efficiency optimization algorithms provide fast and smooth control of stator flux, but they usually require machine parameters and their computational loads is relatively high.

In addition to control algorithm, machine design has also an important effect on the final efficiency of electrical drive. Efficiency maps are usually used to describe the generated losses of an electrical motor with respect to a particular speed/torque. In permanent magnet machines, power losses can be divided into winding (copper) losses and core (iron) losses [10-11].

Comparing to induction machines, core losses in PM motors stand for a larger portion of the total losses. A three-term core-loss model is used in [12-13] to calculate the generated core losses of a PM machine. In [12] [14] the flux density waveforms are estimated in stator tooth and yoke, and some analytical expressions are derived to calculate hysteresis loss and eddy-current loss. However, these approaches are usually used in the design procedure of PM machines where iron losses should be calculated many times

Digital Object Identifier 10.4316/AECE.2014.02023

while executing the design algorithms.

Finite-element methods (FEM) are used in [13] and [15] to precisely calculate tangential and radial flux densities within the stator core and to calculate hysteresis and eddy current loss of each element. The ratio between winding and core losses is a key factor in determining the maximum efficiency point of an electrical motor. While having a constant-speed application, this point can be considered in the design procedure of electrical motor.

Fault tolerant concept is an important issue in applications where the process cannot be stopped due to additional cost penalties or safety reasons [16]. PM drive faults can be generally categorized as actuator faults, airgap irregularities, rotor magnet faults, and stator winding faults [17]. Among these categories, stator winding open-circuit fault and semiconductor failures are the most common ones [18]. Fault tolerant inverter topologies are considered in many papers. In many studies, an additional leg is implemented in inverter configuration to be replaced with the faulty inverter leg, or to feed the machine´s neutral point [19].

Compared with standard three-phase systems, five-phase motor drives present better fault tolerant capabilities. These systems are able to maintain operational in the case of one or even two faulty phases [11] [16] [20-21]. Fault tolerant capability can be achieved by means of modifying stator reference currents and inverter topology.

In [18] [22-23] stator reference currents are optimized to improve the generated output torque of five-phase PM machines and at the same time to limit the stator ohmic losses of each winding to its 1 pu. Although the calculation methods of these studies are quite different, but the resultant values of reference currents are in common.

In this study the efficiency of a fault-tolerant five-phase BLDC drive is evaluated for healthy and different faulty conditions. Open-circuit fault is considered for one, two-adjacent and two-nonadjacent stator phases, and in each case, optimized reference current values of [18] [23] are used to drive the faulty machine. Copper loss and switching loss are calculated by analytical simulations in MATLAB, and stator core losses are computed by FEM simulations in Flux. Different speed values are considered in the efficiency evaluation of five-phase drive. Automotive applications are kept in mind and experimental tests are conducted on an outer-rotor in-wheel type of five-phase BLDC machine with a two-layer winding configuration.

The remaining parts of the paper are organized as follows. In section II, general structure of selected BLDC machine is explained, its electrical model is derived, and its optimized current references under different faulty conditions are introduced. Section III is dedicated to theoretical calculation of different loss sources in BLDC drive and their simulations. Experimental evaluation of developed theories is presented in section IV, and finally, the conclusions extracted from this study are summarized in section V.

II. BLDC Machine Structure and Drive Losses

A general structure of BLDC machines with an outer-rotor topology and a two-layer stator winding is considered in this paper. In this section, BLDC machine model is extracted on the assumption of having a symmetric five-phase winding configuration, and P poles. Let us start with the general equation of machine´s electrical dynamics:

$$[V_s] = r_s[I_s] + \frac{d}{dt}[\Lambda_s] \tag{1}$$

where V_s is voltage matrix of stator winding terminals, r_s and I_s are resistance and current respectively. Λs is the magnetic flux linkage of stator windings which is generated by stator currents and rotor magnets.

$$\Lambda_s = L_{ss} I_s + \Lambda_{PM} \tag{2}$$

where L_{ss} represents stator inductance matrix.

The magnetic flux of rotor magnets in a BLDC machine airgap can be estimated by its first and third harmonic components:

$$\Lambda_{PM} = \lambda_{pm1}\begin{bmatrix} \sin(\theta) \\ \sin(\theta-\frac{2\pi}{5}) \\ \sin(\theta-\frac{4\pi}{5}) \\ \sin(\theta-\frac{6\pi}{5}) \\ \sin(\theta-\frac{8\pi}{5}) \end{bmatrix} + \lambda_{pm3}\begin{bmatrix} \sin(3\theta) \\ \sin 3(\theta-\frac{2\pi}{5}) \\ \sin 3(\theta-\frac{4\pi}{5}) \\ \sin 3(\theta-\frac{6\pi}{5}) \\ \sin 3(\theta-\frac{8\pi}{5}) \end{bmatrix} \tag{3}$$

where λ_{pm1} and λ_{pm3} are first and third harmonic component of rotor magnetic flux, and $\theta = wt$ is rotor electrical angle. Electrical parameters of stator windings can be transferred into synchronous rotating frames which under normal (healthy) conditions result in a simpler and more conceptual control in a DC environment. Considering first and third harmonics, the transformation equation is written in (4) at the beginning of the next page. Using this transformation, stator voltages and currents will be transferred into $d_1 - q_1$ and $d_3 - q_3$ planes which respectively rotate at synchronous speed, and its third multiple.

$$F_{d_1 q_1 d_3 q_3 o} = T\, F_{abcde}$$

$$T_{dqo}(wt) = \frac{2}{5}\begin{bmatrix} \cos(\omega t) & \cos(\omega t - 2\pi/5) & \cos(\omega t - 4\pi/5) & \cos(\omega t - 6\pi/5) & \cos(\omega t - 8\pi/5) \\ -\sin(\omega t) & -\sin(\omega t - 2\pi/5) & -\sin(\omega t - 4\pi/5) & -\sin(\omega t - 6\pi/5) & -\sin(\omega t - 8\pi/5) \\ \cos 3(\omega t) & \cos 3(\omega t - 2\pi/5) & \cos 3(\omega t - 4\pi/5) & \cos 3(\omega t - 6\pi/5) & \cos 3(\omega t - 8\pi/5) \\ -\sin 3(\omega t) & -\sin 3(\omega t - 2\pi/5) & -\sin 3(\omega t - 2\pi/5) & -\sin 3(\omega t - 2\pi/5) & -\sin 3(\omega t - 2\pi/5) \\ 1/\sqrt{2} & 1/\sqrt{2} & 1/\sqrt{2} & 1/\sqrt{2} & 1/\sqrt{2} \end{bmatrix} \tag{4}$$

Multiplication of (1) by T results in the related electrical equations of BLDC machine in two reference frames. These equations can be summarized as:

$$V_{ds1} = r_s i_{ds1} - \omega\lambda_{qs1} + \frac{d\lambda_{ds1}}{dt} \quad (5)$$

$$V_{qs1} = r_s i_{qs1} + \omega\lambda_{ds1} + \frac{d\lambda_{qs1}}{dt} \quad (6)$$

$$V_{ds3} = r_s i_{ds3} - 3\omega\lambda_{qs3} + \frac{d\lambda_{ds3}}{dt} \quad (7)$$

$$V_{qs3} = r_s i_{qs3} + 3\omega\lambda_{ds3} + \frac{d\lambda_{qs3}}{dt} \quad (8)$$

where r_s is the stator resistance, and ω is the electrical rotational velocity. These equations will be used in vector control of BLDC motor. Generated electrical torque will be calculated as:

$$T_e = \frac{5}{2}\frac{P}{2}\left[\lambda_{m1} i_{qs1} + 3\lambda_{m3} i_{qs3}\right] \quad (9)$$

TABLE I. OPTIMIZED STATOR PHASE CURRENTS OF FIVE-PHASE BLDC MACHINE UNDER DIFFERENT FAULTY CONDITIONS [22-23]

Currents	A	B	C	D	E
one faulty phase					
I_1 (pu)	0	0.99	0.99	1	0.98
θ_1°	-	51	137	232	-41
I_3 (pu)	0	0.17	0.08	0.09	0.19
θ_3°	-	23	52	186	-19
two adjacent faulty phases					
I_1 (pu)	0	0	0.59	0.95	0.67
θ_1°	-	-	82	218	1
I_3 (pu)	0	0	0.12	0.29	0.16
θ_3°	-	-	44	102	41
two nonadjacent faulty phases					
I_1 (pu)	0	0.99	0	0.98	0.99
θ_1°	-	77	-	197	-42
I_3 (pu)	0	0.16	0	0.19	0.17
θ_3°	-	15	-	55	-21

Several studies have focused on optimization of amplitude and phase angle of current references under faulty conditions. In almost all of these studies, rated RMS value of phase copper losses is considered as a limit in the optimization process to avoid thermal stress (hot spots) within the stator core. Moreover, it is tried to increase the output power, while limiting the generated torque ripples. Optimization procedure of stator reference currents under different conditions is beyond the scope of this paper. Table I presents the desired reference current values which are globally optimized by genetic algorithm in [23] and analytically computed in [24] for a five-phase BLDC machine.

III. LOSS SIMULATION

Simulations are conducted to evaluate the stator core (iron) losses, stator winding (copper) losses, and inverter switching losses. Each of these aspects will be explained in the following subsections.

A. Stator Core (Iron) Losses

Iron losses can play an important role in generated thermal stresses of stator core. However, as stator core losses are a function of used material, winding configuration and machine design, it is not possible to generally optimize the reference values of stator phase currents for all types of five-phase BLDC machines under faulty conditions. In this paper, optimized values of stator currents are used to evaluate both copper and iron losses of an outer-rotor five-phase BLDC machine.

Stator core losses W_t can be divided into three categories of hysteresis losses W_h, eddy current losses W_e, and anomalous (or excess) losses W_e [10][25]:

$$W_t = W_h + W_e + W_f \quad (10)$$

Hysteresis losses of the stator core can be calculated as:

$$W_h = k_h B_{\max}^2 f \quad (11)$$

where k_h is the experimental coefficient of magnetic losses due to hysteresis [WsT^2m^3], B_{max} is the peak value of magnetic flux density [T], and f represents the electrical frequency [Hz] [10] [26]. In addition, the losses related with induced eddy currents can be computed as:

$$W_e = \frac{\pi^2 \sigma d^2}{6} B_{\max}^2 f^2 \quad (12)$$

where σ is the electrical conductivity of implemented ferromagnetic material [S/m], and d is lamination thickness [m]. Moreover, anomalous power losses can be calculated as:

$$W_a = 8.67 k_e (B_{\max} f)^{1.5} \quad (13)$$

where k_e is the experimental coefficient of anomalous (excess) losses [$W(Ts^{-1})^{-1.5}m^-$]. Assuming the stacking factor of K_f for steel laminations, equation (10) can be written as:

$$W_t = k_f\left[k_h B_{\max}^2 f + \frac{\pi^2 \sigma d^2}{6} B_{\max}^2 f^2 + 8.67 k_e (B_{\max} f)^{1.5}\right] \quad (14)$$

In this equation σ, d and k_f are known values. Moreover, k_h and k_e can be provided by lamination´s manufacturer. As a result, equation (14) can be used to compute stator iron losses [10][25].

To compute stator iron losses, FEM simulations are conducted in two dimensions by Flux-Cedrat® software. Simulation sampling frequency is set on 4.9 kHz, and the total numbers of simulated points are set to 2048. Stator winding configuration is similar to Fig. 1 but with 26 pole-pairs. Stator winding configuration, core laminations, and applied 2D mesh plot of the simulations are presented in Fig. 1.

Non-oriented electrical steel M235-35A laminations are considered in the simulation which corresponds to the implemented material in the real test bench. Specific losses of soft ferromagnetic materials include hysteresis losses, eddy losses and excess losses. Figure 2 shows the specific losses of M235-35A steel as a function of magnetic polarization. This information is provided by manufacturer at f_e = 100 Hz and f_e = 200 Hz. By applying interpolation, specific losses of these laminations can be computed for the

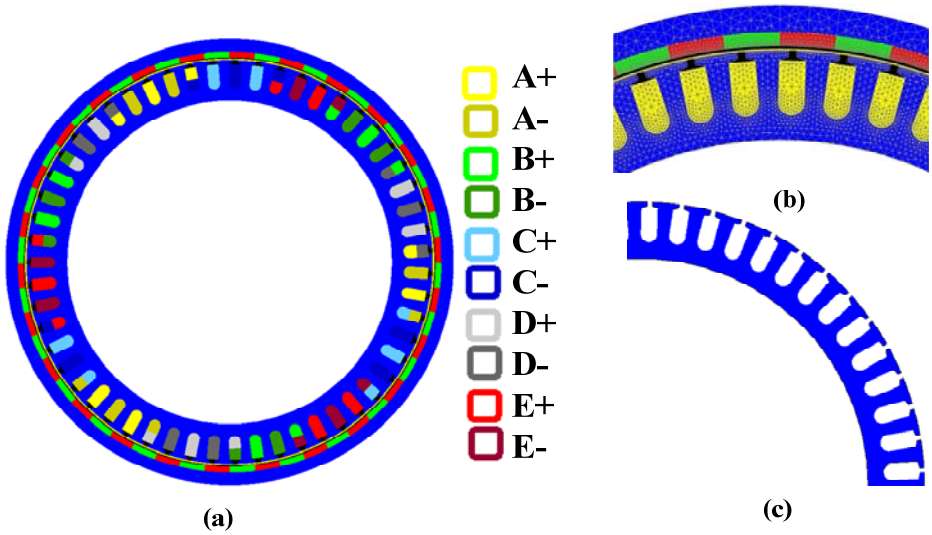

Figure 1. Five-phase BLDC machine stator, (a) winding configuration, (b) 2D mesh plot, (c) stator core lamination

rated frequency of five-phase BLDC machine in the test bench (f_e = 173 Hz). Figure 2 presents the specific losses of M235-35A steel as a function of peak value of magnetic flux density. As a result, by extracting the information of two separate points in Fig. 2, it is possible to compute the experimental coefficients of k_h and k_e at rated frequency of 173 Hz. Physical properties of simulated laminations are summarized in Table II.

The derived coefficients are used in FEM simulations to calculate stator core losses while the machine is rotating at its rated speed. Table III presents the simulated values of stator core losses for five-phase BLDC machine under healthy and different faulty conditions. As it can be seen from Table III, in the case of missing one phase, $P_{loss\text{-}iron}$ is less than its value in normal conditions. In fact, if reference currents were not modified and stator windings were physically separated, then iron losses due to stator currents should be reduced to 80% its rated value. However, $P_{loss\text{-}iron}$ is reduced to 84% of its value under normal conditions.

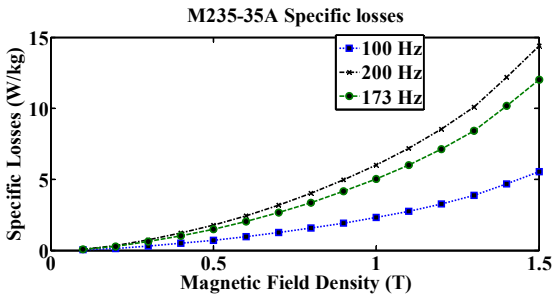

Figure 2. Specific losses of steel lamination as a function of magnetic field density

TABLE II. PHYSICAL PROPERTIES OF STEEL LAMINATIONS

Parameter	Value
Electrical Conductivity, σ	$1.695.10^6\, Sm^{-1}$
Density, ρ	$7850 kgm^{-3}$
Thickness, d	$0.35.10^{-3}\, m$
Hysteresis coefficient, k_h	$67.38100 WsT^{-2}m^{-3}$
Excess losses coefficient, k_e	$0.95211 W(Ts^{-1})^{-1.5}m^{-3}$
Stacking factor, k_f	0.96

TABLE III. STATOR IRON LOSSES OF FIVE-PHASE BLDC MACHINE AT ITS RATED SPEED

Motor Condition	Stator core (iron) losses (pu)
Normal (Healthy)	0.06
One missing phase	0.0504
Two adjacent missing phases	0.0456
Two non-adjacent missing phases	0.0432

This higher value of losses is due to double-layer configuration of stator winding which leads to iron loss in all regions of stator core. Moreover, although the RMS value of stator phase currents is still 1 pu, but the peak value of optimized reference currents has increased by 10% in two of the remaining stator phases which increases the saturation level of implemented laminations. In addition, rotor magnetic field does not depend on stator winding currents and generates a constant value of iron losses in the stator.

In the case of missing two adjacent faulty phases, $P_{loss\text{-}iron}$ is 76% of its value under normal conditions. Again, in the case of separated windings and no modification in stator reference currents, the expected value of $P_{loss\text{-}iron}$ due to stator currents should be 60% its rated value.

However, to generate a ripple-free torque, the stator phase currents should be adapted. In fact, in this case the peak value of stator phase currents are $I_{C\text{-}peak}$ =0.68 pu, $I_{D\text{-}peak}$ = 1.24 pu, and $I_{E\text{-}peak}$ = 0.68 pu. High value of $I_{D\text{-}peak}$, double-layer configuration of stator windings, and constant value of rotor magnetic field are the main reasons of higher core losses in the case of missing two adjacent phases.

In the case of missing two non-adjacent phases, the physical situation of the remaining healthy phases are quite symmetric, and peak values of stator reference currents are $I_{B\text{-}peak} \approx 0.88$ pu, $I_{D\text{-}peak} \approx 1.12$ pu, and $I_{E\text{-}peak} \approx 1.12$ pu. Under this operational condition, $P_{loss\text{-}iron}$ is 72% of its value while operating under normal conditions. Comparing to the case of having two adjacent missing phases, stator current peak values are more moderated. However, again peak values of stator reference currents are more than 1 pu in two of the remaining phases. As it can be seen in this case $P_{loss\text{-}iron}$ is 4% less than its value in the case of missing two adjacent faulty phases which is firstly due to a reduction in maximum peak value of stator current in the remaining healthy phases, and secondly, more uniform distribution of remaining phase

windings.

B. Stator Winding (Copper) Losses

Stator copper losses in the remaining healthy phases can be simply calculated as:

$$p(t) = v(t)i(t) = ri^2(t) \quad (15)$$

Using the reference values of [22] and by knowing that $r_s = 0.1\,\Omega$, pu values of generated copper loss in stator windings are summarized in Fig. 3 for each condition.

RMS value of stator phase currents is the main limiting factor in the optimization procedure of stator reference currents while missing one or two stator phases. In the case of missing one stator phase, copper losses are 1 pu in the remaining healthy phases, and total amount of stator copper losses is 80% of its value under normal operation.

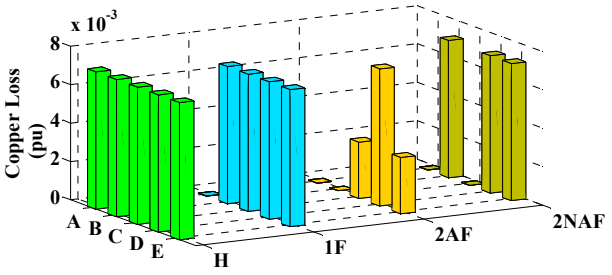

Figure 3. pu values of stator copper loss under healthy condition (H) and while missing one phase (1F), two adjacent phases (2AF) and two non-adjacent phases (2NAF)

While missing two adjacent stator phases, stator copper losses are less in the two non-adjacent remaining phases. The main reason of this fact is torque ripple constraints in the optimization procedure of stator reference currents. In other words, to generate a ripple-free torque in the case of missing two-adjacent phases, it is not possible to use the entire copper capacity of the remaining three healthy windings. The entire copper losses under this condition is 37% its value under normal operation.

C. Inverter Losses

As it was mentioned previously, off-state losses are not considered in this study. To calculate the conduction losses, IGBT and diode models are considered as voltage sources with a resistor in series. The average value of conduction losses during the modulation period T can be computed as:

$$P_{cond} = \frac{1}{T}\int_0^T (V_{Fo} + R_{on} i_F) i_F \, dt \quad (16)$$

where V_{Fo}, i_F and R_{on} are respectively threshold voltage, forward current and dynamic resistance of semiconductors. The main reason of switching losses is non-ideal characteristics of IGBTs during turn-on and turn-off moments (switching instants). As a result, switching losses are directly dependent on inverter switching frequency and modulation period. Average value of switching losses in one modulation period can be calculated as [24]:

$$P_{sw} = \frac{1}{T}\sum_{j=1}^{n}\left[E_{on}(i_F, v_{off}) + E_{off}(i_F, v_{off}) + E_{rec}(i_F, v_{off})\right] \quad (17)$$

where n is the number of transitions in each switching period, E_{on}, E_{off} and E_{rec} are turn-on, turn-off and reverse recovery losses of IGBT switch, and T is the fundamental period of drive component. To simulate the inverter losses, it is required to formulate dynamic and static characteristics of implemented IGBTs and diodes. These characteristics include turn-on and turn-off energy and voltage drop of each semiconductor.

These characteristics are formulated by using datasheet information of inverter semiconductors and MATLAB Curve Fitting toolbox. Table IV presents the derived polynomial functions of FP15R06W1E3 IGBT model and their reverse diodes.

TABLE IV. ESTIMATED DATA FOR FP15R06W1E3

	Estimated characteristic
	Transistor
Voltage drop	$0.1056\times i^{0.4602} + 0.3161$
Turn on Energy: E_{on}(mJ)	$0.0001723\times i^2 - 0.02001\times i + 7.423$
Turn off Energy: E_{off}(mJ)	$0.0936\times i + 3.2687$
	Diode
Voltage drop	$0.6781\times i^{0.2387} - 0.2912$
Turn off Energy: E_{off}(mJ)	$63\times\exp(-0.001732\times i) - 58.3\times\exp(-0.0029\times i)$

Moreover, Fig. 4 illustrates the simulated losses of inverter block. Five-phase BLDC drive is simulated and inverter losses are computed (in watts) for steady states and under healthy and each faulty condition. In the case of healthy conditions, total amount of conduction and switching losses in each leg is 0.83 % of the rated power. In this case, conduction losses and switching losses are equal for all inverter legs.

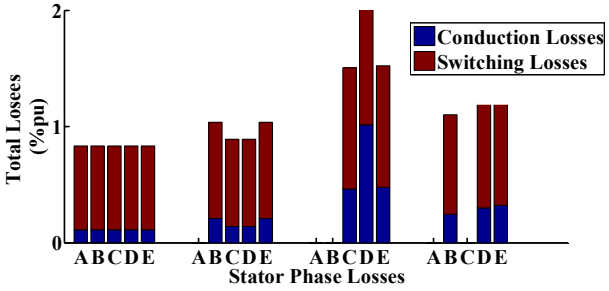

Figure 4. Simulated values of conduction and switching losses of five-phase inverter under healthy and different faulty conditions

While missing one stator phase, both switching and conduction losses increase in the remaining inverter legs. Under this condition, $I_{B\text{-}peak}$=1.12 pu, $I_{C\text{-}peak}$=1.00 pu, $I_{D\text{-}peak}$=1.00 pu, and $I_{E\text{-}peak}$=1.12 pu. As a result, it is expected that the losses increase more in phases B and E. comparing to the healthy case, conduction loss increment of phase B and E is 0.10% rated power. Moreover, switching loss increment is 0.10% rated power. The increment of both conduction and switching losses for the remaining two phases is 0.028 % rated power.

In the case of missing two adjacent phases, both conduction and switching losses increase in the remaining three phases. Comparing to normal (healthy) operation, the increment of conduction losses in phases C, D and E are respectively 0.35%, 0.90% and 0.36% of the rated power. The increment of switching losses for phases C, D and E are 0.32%, 0.72% and 0.32% rated power, respectively. As it can be seen from Fig. 5, inverter losses are higher in leg D of the inverter which is due to higher peak value of stator currents in its corresponding phase.

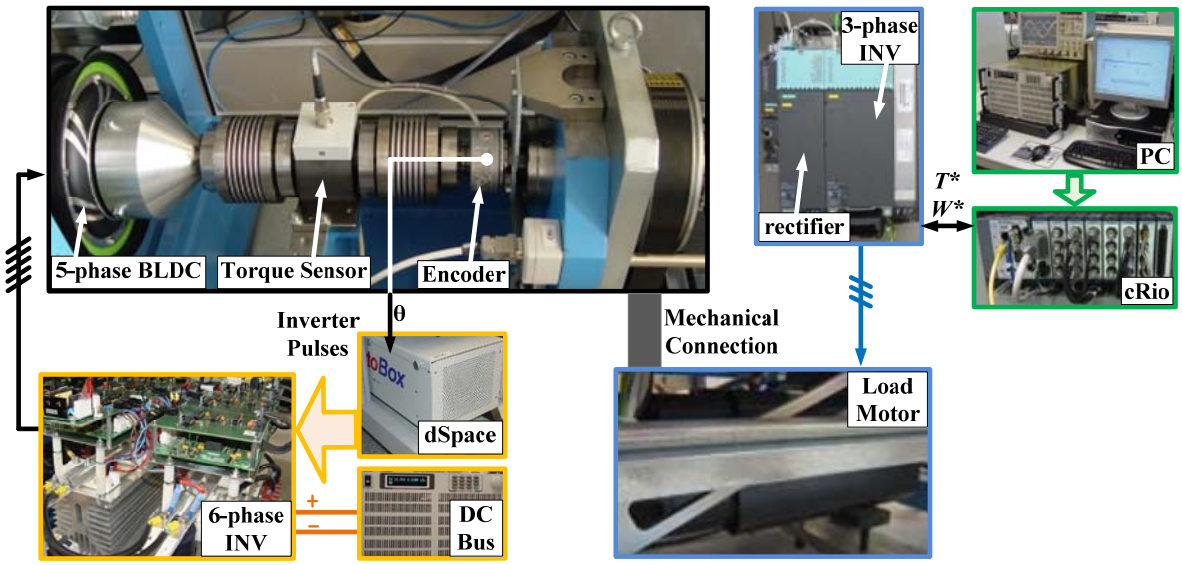

Figure 5. Test bench configuration

On the other hand, while missing two non-adjacent phases, stator phase currents are more symmetric. As a result, comparing to the case of missing two adjacent faulty phases, the switching losses are less in this case. Comparing to normal operation, the conduction loss in phases B, D and E have an increment of 0.13%, 0.19% and 0.21% of the rated power. Moreover, switching loss increment in each one of these cases is 0.14%, 0.17% and 0.19% of the rated power.

IV. Experimental Evaluation

To evaluate the theoretical investigations, experimental tests are conducted on a commercial type of five-phase BLDC hub motor. Figure 5 presents the general configuration of the test bench. The stator incorporates a double-layer fractional-slot winding accompanied by an outer-rotor. Due to its high number of pole pairs, the magnets are simply installed on rotor inner surface. Machine´s parameters are summarized in Table V.

Motor phase terminals are fed by a five-phase inverter with a 48V dc-bus and 5 kHz of switching frequency. In addition, stator current controlling algorithm is realized by DS1005 dSpace board, and mechanical speed is controlled (fixed) by the load system. Under each operational condition, real and reference values of stator phase currents are compared, and the resultant current errors are used in controllers to calculate the required reference voltages of each phase. Under faulty conditions, stator phase currents are directly controlled in phase reference coordination. Proportional-resonant (PR) controllers are used to calculate the reference values of phase terminal voltages [27].

An incremental encoder and 5 Hall Effect sensors are used to close the position and current loops. Load system is a commercial three-phase PMSM which is driven independently by a three-phase AC drive (famous as SINAMICS S120). A real-time controller (known as cRio) is used as an interference between host computer and three-phase inverter. Constructed five-phase inverter and the mechanical link between load and five-phase BLDC motor are also shown in Fig. 5. In addition, stator currents under healthy and each faulty condition are summarized in Fig. 6. The computational power of implemented dSpace and its IO port speed are limited. As a result, 5 kHz is the maximum achievable switching frequency. It is worth noting that due to relatively low value of motor speed, air friction losses and ball bearing losses are negligible. As a result, these sources of losses are not considered in simulation evaluations.

In each case, input and output power of BLDC drive are measured under steady state to evaluate the efficiency of BLDC drive. Input power is directly calculated by measuring the output current of dc power supply and multiplying it by dc bus voltage. On the other hand, to compute the output power of five-phase BLDC drive, mechanical torque is measured in healthy and different faulty conditions. Table VI summarizes the measured values of input and output power for each case.

While operating under normal conditions, the measured efficiency value of the entire drive is 88.4% which is close to its simulated value (87.9%). regarding simulation results,

Table V. Electrical (measured) parameters of five-phase BLDC machine

Parameter		value
Number of Pole Pairs		26
Stator Resistance		0.1 Ω
Stator Inductance	L_{aa}	408 *uH*
	L_{ab}	15 *uH*
	L_{ac}	18 *uH*
Nominal Torque		8 *Nm*
Nominal Power		350 Watt
Nominal Phase Current		5 Amp (rms)
Nominal Phase Voltage		16 V (rms)
DC-bus Rated Voltage		48 V
Nominal Speed		400 *rpm*
Permanent Magnet Flux		0.0178 *Wb*

TABLE VI. MEASURED VALUES OF BLDC DRIVE INPUT AND OUTPUT POWERS AND ITS EFFICIENCY

Condition	$P_{in\text{-}elec}$ (pu)	$P_{out\text{-}mech}$ (pu)	$P_{loss\text{-}tot}$ (pu)	Eff.
Normal (H)	1.13	1	0.13	0.88
1F	0.86	0.73	0.13	0.84
2AF	0.39	0.26	0.13	0.66
2NAF	0.66	0.55	0.11	0.83

while working with a healthy machine the main part of BLDC drive losses are related to iron core (0.06 pu), and after that, inverter unit losses (0.04 pu) and stator windings copper losses (0.03 pu).

Comparing to normal operation, the measured value of drive efficiency is less in the case of missing one stator phase (84%). In this case, the maximum value of output power is reduced to 0.73 pu [23], and as the RMS value of stator currents in the remaining healthy phases is kept on 1 pu, stator copper losses are 80% their rated value. Stator current peak values are higher than 1 pu in two of the remaining phases which results in higher amplitudes of conduction and switching losses in their correspondent inverter legs. Regarding the simulations, in this case the main part of BLDC drive losses are again generated by stator iron core (0.05 pu), and after that, inverter unit losses (0.04 pu) and stator copper losses (0.028 pu) are the most important reasons of efficiency reduction in the drive.

In the case of missing two adjacent phases, measured drive efficiency decreases down to 66% which is highly noticeable comparing to its value under normal conditions (88%). The main reason of this efficiency reduction is related to optimized values of stator reference currents under this condition [22-23]. In fact to limit the generated ripples in the case of missing two adjacent phases, fundamental component of stator currents should be less than 0.7 pu in two non-adjacent healthy phases, and high amplitudes of third harmonic components are required. Moreover, theoretical value of ripple-free output power is reduced to 0.27 pu. In this case, the main parts of BLDC drive losses are related to the inverter losses (0.0548 pu) which is due to high peak value of stator currents. After inverter losses, stator core losses (0.04 pu) is the biggest source of power losses in BLDC drive. In addition, as it is not possible to use the entire copper capacity of the remaining healthy phases, stator copper losses are reduced to 0.013 pu in this case.

In the case of missing two non-adjacent stator phases, the measured value of BLDC drive efficiency is 83% which is close to its simulated value (84.7%). Comparing to the case of two adjacent faulty phases, there is a noticeable increment in final value of drive efficiency. The main reason of higher efficiency is more symmetric situation of the remaining healthy phases which allows having a better utilization of stator copper capacity to generate more ripple-free output power. The maximum achievable output power in this case is limited to 0.55 pu which is due to keeping the RMS value of stator reference current under 1 pu. Regarding simulations, in this case, the main source of BLDC drive losses are related to stator core iron (0.04 pu), and after that

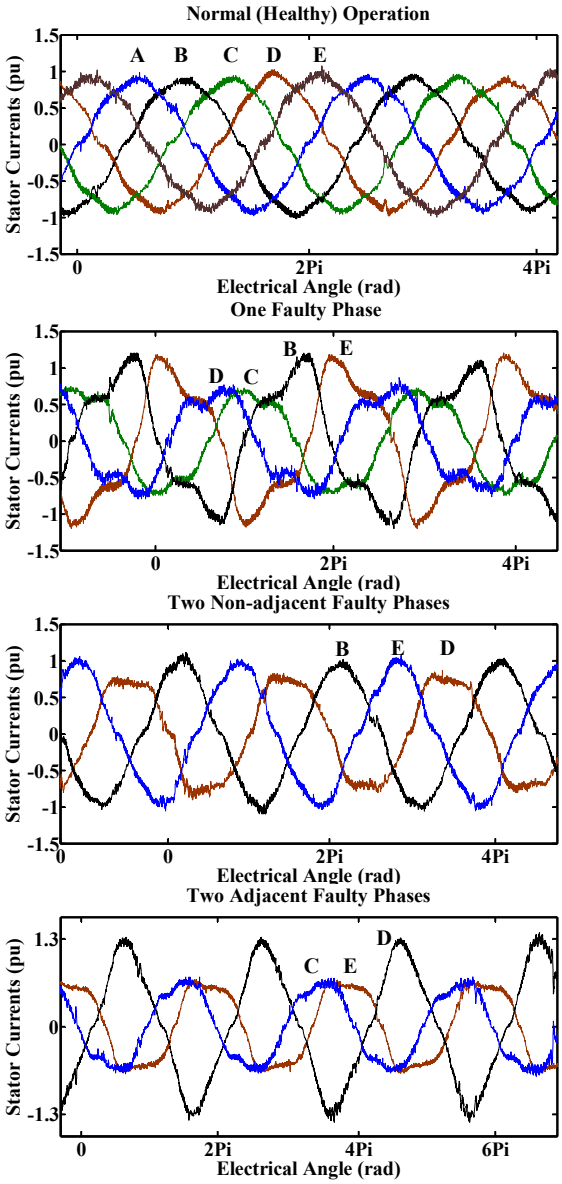

Figure 6. Stator phase currents under healthy and various faulty conditions

inverter block losses (0.03 pu) and stator copper losses (0.02 pu) are the most important reasons of efficiency reduction.

V. CONCLUSION

In this paper, the efficiency of a fault tolerant five-phase PM drive is evaluated. Considered machine is a five-phase outer-rotor BLDC motor with a double-layer winding configuration. Open-circuit fault is considered in one, two adjacent and two non-adjacent stator phases. In each case, RMS value of stator reference currents is the main limiting constraint of generated ripple-free torque. Stator core losses are calculated by means of simulations in Flux-Cedrat® environment. It is shown that iron losses are the most important part of BLDC drive losses under normal operation and while missing one phase and two non-adjacent phases. In addition, inverter unit losses and stator winding (copper) losses are simulated in MATLAB environment. In the case of having two adjacent faulty phases, inverter losses are the most important reason of BLDC drive losses. Regarding simulations, the final efficiency of BLDC drive is 87%, 86%, 70% and 84% respectively in the case of working with

a healthy machine, a machine with one missing phase, a machine with two adjacent missing phases, and a machine with two non-adjacent missing phases. In addition, experimental tests are conducted to verify the simulation results. Measured value of BLDC drive efficiency is 89%, 84%, 66% and 83% respectively in the case of working with a healthy machine, and while missing one phase, two adjacent phases and two non-adjacent phases.

REFERENCES

[1] D. Ha, C. Lim, D. Hyun, "Robust optimal nonlinear control with observer for position tracking of permanent magnet synchronous motors," Journal of Power Electronics, vol. 13, no. 6, pp. 975-984, Nov. 2013.

[2] J. Yu, H. Cho, J. Choi, S. Jang, S. Lee, "Optimum design of stator and rotor shape for cogging torque reduction in interior permanent magnet synchronous motors," Journal of Power Electronics, vol. 13, no. 4, pp. 546-551, Nov. 2013.

[3] D. Nguyen, H. Lee, T. Chun, "A carrier-based pulse width modulation method for indirect matrix converters," Journal of Power Electronics, vol. 12, no. 3, pp. 448-457, Nov. 2012.

[4] J. Abu Qahouq, V. Arikatla, T. Arunachalam, "Modified digital pulse width modulator for power converters with a reduced modulation delay," Journal of Power Electronics, vol. 12, no. 1, pp. 98-103, Jan. 2012.

[5] T.W. Jian, N. L. Schmitz, D.W. Novotny, "Characteristic induction motor slip values for variable voltage part load performance optimization," IEEE Trans. Power App. Syst., vol. PAS-102, no. 1., pp. 38–46, Jan. 1983.

[6] H. G. Kim, S. K. Sul, M. H. Park, "Optimal efficiency drive of a current source inverter fed induction motor by flux control," IEEE Trans. Ind. App., vol. IA-20, no. 6, pp. 1453–1459, Nov./Dec. 1984.

[7] A. Kusko, D. Galler, "Control means for minimization of losses in AC and DC motor drives," IEEE Trans. Ind. App., vol. IA-19, no. 4, pp. 561–570, July/Aug. 1983.

[8] F. Abrahamsen, F. Blaabjerg, J. K. Pedersen, P. Grabowski, P. Thoegersen, "On the energy optimized control of standard and high-efficiency induction motor in CT and HVAC applications," IEEE Trans. Ind. App., vol. 34, no. 4, pp. 822–831, July/Aug. 1998.

[9] K. S. Rasmussen, P. Thoegersen, "Model based energy optimizer for vector controlled induction motor drives," in Proc. EPE'97, 1997, pp. 3.711–3.716.

[10] G. Bertotti, "General properties of power losses in soft ferromagnetic materials," IEEE Trans. Magn., vol. 24, no. 1, pp. 621-630, Jan. 1988.

[11] L. Parsa, H. A. Toliyat, "Five-phase permanent-magnet motor drives," IEEE Trans. Ind. App., vol. 41, no. 1, Jan./Feb. 2005.

[12] G. R. Slemon, L. Xian, "Core losses in permanent magnet motors," IEEE Trans. Magn., Vol. 26, No. 5, pp. 1653–1655, Sep. 1990.

[13] K. Yamazaki, H. Ishigami, "Rotor-shape optimization of interior-permanent-magnet motors to reduce harmonic iron losses," IEEE Trans. Ind. Electron., vol. 57, no. 1, pp. 61–69, Jan. 2010.

[14] W. Jiabin, T. Ibrahim, D. Howe, "Prediction and measurement of iron loss in a short-stroke, single-phase, tubular permanent magnet machine,"IEEE Trans. Magn., vol. 46, no. 6, pp. 1315–1318, Jun. 2010.

[15] K. Atallah, Z. Q. Zhu, D. Howe, "An improved method for predicting iron losses in brushless permanent magnet DC drives," IEEE Trans. Magn., vol. 28, no. 5, pp. 2997–2999, Sep. 1992.

[16] B. Park, R. Kim, D. Hyun, "Open circuit fault diagnosis using stator resistance variation for permanent magnet synchronous motor drives," Journal of Power Electronics, vol. 13, no. 6, pp. 985-990, Nov. 2013.

[17] L. Romeral, J. C. Urresty, J. R. R. Ruiz, A. G. Espinosa, "Modeling of surface-mounted permanent magnet synchronous motors with stator winding interturn faults," IEEE Trans. Ind. Elect., vol. 58, no. 5, pp. 1576-1585, May 2011.

[18] A. Mohammadpour, L. Parsa, "A unified fault-tolerant current control approach for five-Phase PM motors with trapezoidal back-EMF under different stator winding connections," IEEE Trans. Power Elect., vol. 28, no. 7, pp. 3517-3527, Jul. 2013.

[19] R. Brian, A. Welchko, T. A. Lipo, T. M. Jahns, S. E. Schulz, "Fault tolerant three-phase AC motor drive topologies: a comparison of features, cost, and limitations," IEEE Trans. Power Electron., vol. 19, no. 4, pp. 1108-1116, Jul. 2004.

[20] B. Park, K. Lee, R. Kim, D. Hyun, "Low-cost fault diagnosis algorithm for switch open-damage in BLDC motor drives," Journal of Power Electronics, vol. 10, no. 6, pp. 702-708, Nov. 2010.

[21] A. Jack, B. Mecrow, J. Haylock, "A comparative study of permanent magnet and switched reluctance motors for high-performance fault tolerant applications," IEEE Trans. Ind. App., vol. 32, no. 4, Jul. 1996.

[22] S. Dwari, L. Parsa,"Fault-tolerant control of five-phase permanent-magnet motors with trapezoidal back-EMF," IEEE Trans. Ind. Electron., vol. 58 , no. 2, pp- 476 – 485, Feb. 2011.

[23] R. Salehi Arashloo, J. L. Romeral Martinez, M.Salehifar, M. Moreno-Eguilaz, "Genetic algorithm based output power optimization of fault tolerant five-phase BLDC drives applicable for electrical and hybrid electrical vehicles," IET Journal on Electric Power Applications, April 2014.

[24] N. Bianchi, S. Bolognani, M. Pré, E. Fornasiero, "Post-fault operations of five-phase motor using a full-bridge inverter," IEEE Power Electron. Specialists Conf., pp. 2528–2534, Jun. 2008.

[25] H. Saavedra, J. Riba, L. Romeral, "Inter-turn fault detection in five-phase pmsms. Effects of the fault severity," IEEE symposium, Diagnostics for Electric Machines, Power Electronics and Drives (SDEMPED), pp. 520-526, Aug. 2013.

[26] J. Siahbalaee, S. Vaez-Zadeh, F. Tahami, "A loss minimization control strategy for direct torque controlled interior permanent magnet synchronous motors," Journal of Power Electronics, vol. 9, no. 6, pp. 940-948, Nov. 2009

[27] R. C´ardenas, C. Juri, R. Pe˜na, P. Wheeler, J. Clare, "The application of resonant controllers to four-leg matrix converters feeding unbalanced or nonlinear loads," IEEE Trans. Power Electron., vol. 27, no. 3, pp. 1120 – 1129, March 2012.